SCIENTIFIC REPORTS
nature research

OPEN

A kinetic method for measuring agonist efficacy and ligand bias using high resolution biosensors and a kinetic data analysis framework

Sam R. J. Hoare[1,3*], Paul H. Tewson[2,3], Anne Marie Quinn[2] & Thomas E. Hughes[2*]

The kinetics/dynamics of signaling are of increasing value for G-protein-coupled receptor therapeutic development, including spatiotemporal signaling and the kinetic context of biased agonism. Effective application of signaling kinetics to developing new therapeutics requires reliable kinetic assays and an analysis framework to extract kinetic pharmacological parameters. Here we describe a platform for measuring arrestin recruitment kinetics to GPCRs using a high quantum yield, genetically encoded fluorescent biosensor, and a data analysis framework to quantify the recruitment kinetics. The sensor enabled high temporal resolution measurement of arrestin recruitment to the angiotensin AT_1 and vasopressin V_2 receptors. The analysis quantified the initial rate of arrestin recruitment (k_τ), a biologically-meaningful kinetic drug efficacy parameter, by fitting time course data using routine curve-fitting methods. Biased agonism was assessed by comparing k_τ values for arrestin recruitment with those for Gq signaling via the AT_1 receptor. The k_τ ratio values were in good agreement with bias estimates from existing methods. This platform potentially improves and simplifies assessment of biased agonism because the same assay modality is used to compare pathways (potentially in the same cells), the analysis method is parsimonious and intuitive, and kinetic context is factored into the bias measurement.

The kinetics/dynamics of G-protein-coupled receptor (GPCR) signaling is of increasing interest in elaborating the biology and therapeutic potential of these receptors[1–3]. The time frame of GPCR signal transduction is dependent on the signaling pathway, regulation of signaling mechanism, and location of the receptor in the cell (spatiotemporal signaling). Temporal dynamics of signaling are being elucidated and applied to develop new therapeutics. For example, the parathyroid hormone 1 (PTH1) receptor can signal persistently over time after partitioning into the endosomal compartment[4]. This effect was ligand dependent; PTH produced persistent signaling whereas PTH-related protein did not[4]. This behavior is potentially involved in the therapeutic mode of action; continuous administration of PTH1 receptor agonists results in bone loss, whereas intermittent administration results in net bone formation[5]. This kinetic effect was exploited in the development of new bone anabolic agents for treating osteoporosis[6]. Persistent signaling is potentially beneficial for other GPCR therapeutics[1], for example sphingosine 1-phosphate receptor-1 agonists for treatment of multiple sclerosis[7].

Of potential concern, the kinetics of signaling can affect measurement of biased agonism, by affecting classical measurements of agonist activity (potency and efficacy)[3,8]. Biased agonism is the capacity of a ligand to selectively activate one or more of multiple signaling pathways transduced by the GPCR[9]. This concept is of considerable current interest in the development of next-generation GPCR therapeutics because it enables selective targeting towards beneficial pathways and away from potentially deleterious ones[10–12]. For a series of dopamine receptor ligands, it was shown that the extent of bias was dependent on the time point at which the signaling responses were measured[8]. This complicates the interpretation of bias and its translation to *in vivo* efficacy because it isn't

[1]Pharmechanics LLC, 14 Sunnyside Drive South, Owego, NY, 13827, USA. [2]Montana Molecular, 366 Gallatin Park Dr. Suite A, Bozeman, MT, 59715, USA. [3]These authors contributed equally: Sam R.J. Hoare and Paul H. Tewson. *email: sam.hoare@pharmechanics.com; thughes@montanamolecular.com

straightforward to select the most appropriate time point for establishing structure-activity relationships and for predicting *in vivo* efficacy from *in vitro* bias measurements. Differences in assay timing might contribute to discrepancies of bias estimates reported in the literature. For example, aripiprazole has been reported to be an arrestin-biased ligand but the efficacy varies from 10 to 100% and the time point from 5 minutes to 20 hours[13–17].

Quantifying the kinetics of signaling with useful drug parameters would aid the development of kinetically-optimized molecules, tuned, for example, to the optimum duration of signaling, timeframe of desensitization, and residence period in signaling compartments. This requires appropriately optimized kinetic assays and a data analysis platform for extracting drug parameter values from time course data. Biosensor assays have enabled high-throughput kinetic measurement of GPCR signal transduction because the same plate/well can be measured repeatedly over time[18–20]. The signaling molecule of interest interacts with an engineered protein, changing its optical properties, for example fluorescence intensity, which is detected in specialized plate readers. Previously we and others have developed genetically-encoded biosensors incorporating fluorescent proteins such as mNeonGreen that provide high-resolution kinetic data for G-protein-mediated signals (for example, cAMP[21], diacylglycerol[21] (DAG), and Ca^{2+}[22]). Regarding the data analysis, drug activity metrics are required which quantify the kinetics in terms that can be applied in establishing structure-activity relationships[23]. We recently developed a data analysis framework for G-protein and downstream signaling that quantifies kinetics in terms of the initial rate of signaling[24,25]. This rate, analogous to the initial rate of enzyme activity, is the rate of signaling before it is impacted by regulation of signaling mechanisms such as receptor desensitization and signal decay[25]. This parameter, termed k_τ, provides a biologically meaningful kinetic metric of ligand efficacy that has been applied to quantify ligand activity for G-protein activation and second-messenger generation[24,25].

The goal of this study was to optimize and integrate the biosensor modality and the data analysis framework to create a unified platform suitable for robustly measuring and quantifying signaling kinetics and biased agonism for numerous GPCR pathways. This first required extending the framework described above to arrestin recruitment, since our biosensor and analysis technologies were developed only for G-protein signaling. Arrestin recruitment is an alternative pathway by which GPCRs modulate cellular activity[26,27] and arrestin recruitment has been implicated in potentially beneficial and deleterious physiological processes. For example, arrestin recruitment by the angiotensin AT_1 receptor improves the cardiac performance of ligands targeting the receptor in animal models[28–31], whereas arrestin recruitment by the μ opioid receptor has been implicated in opioid side effects, including tolerance, reward and respiratory depression[32–35]. This has stimulated the development of ligands biased towards or away from the arrestin pathway[9,11,36]. Here we describe a novel arrestin biosensor, utilizing mNeonGreen, suitable for generating time course data with high enough temporal resolution for the arrestin recruitment kinetics to be measured accurately. We then extended the data analysis framework to incorporate arrestin recruitment to the receptor. Finally, we applied this unified platform to directly compare arrestin recruitment and G-protein signaling via the AT_1 receptor, using near-identical experimental conditions and the same conceptual kinetic data analysis framework. This work demonstrated a novel approach for quantifying biased agonism in kinetic terms using a unified assay modality.

Results

In this study an experimental and analytical platform was developed to quantify the kinetics of arrestin recruitment in such a way as to enable direct comparison with the kinetics of downstream signaling. A genetically-encoded biosensor that converts the change in arrestin conformation upon receptor interaction to a change in fluorescence intensity made it possible to collect detailed recordings of the kinetics of arrestin recruitment, i.e. a large number of reads at closely-spaced time points. Robust arrestin responses were obtained for the angiotensin AT_1 and vasopressin V_2 receptors. The time course data, i.e. the change in fluorescence intensity over time, was then analyzed using a novel pharmacological analysis. This analysis quantifies the initial rate of arrestin recruitment to the receptor. The analysis was applied to responses activated by several agonists of the AT_1 angiotensin receptor. Biased agonism was then assessed; the initial rate of arrestin recruitment was compared with the initial rate of downstream signaling measured using the same biosensor modality (DAG generation and Ca^{2+} mobilization). The resulting bias ratios were in good agreement with values obtained using conventional methods, validating the method.

Biosensor of arrestin-receptor interaction. Accurately quantifying signaling over time with an optical biosensor requires certain physical criteria. GPCR signaling is often rapid, for example the rise phase occurs within a few seconds for Ca^{2+} mobilization and within a few minutes for cAMP generation and arrestin recruitment. Consequently, in order to obtain sufficient data points, the read time, the time required to obtain sufficient signal, needs to be short, ideally <10 seconds. Second, a large number of time points are required to accurately define the curve shape and reliably fit the relevant equations to the time course data. This requires minimal photobleaching of the sensor. These criteria can be met with direct fluorescence sensors, owing to the high quantum yield[21,22]. This property enables short read times to be used because the signal per unit time is high. It also minimizes photobleaching because a short excitation time can be used.

We and others have developed fluorescent biosensors in which intrinsically fluorescent protein sensors have been incorporated. (Three examples used in this study are R-GECO[22] for Ca^{2+}, Downward DAG for DAG and cADDis for cAMP[21]). The protein sensors have been engineered to be conformationally-sensitive, such that interaction with the signaling molecule of interest changes the optical properties, enabling the interaction to be detected as a change of fluorescence intensity. Since the proteins are intrinsically fluorescent, no chemical tagging or substrate addition is necessary to generate the optical signal. Here this approach was used to develop a biosensor of receptor-arrestin interaction (Fig. 1a). Arrestin-3 (also known as β-arrestin2) and the fluorescent protein mNeonGreen[37,38] were fused together such that the entire arrestin molecule was inserted into the critical seventh stave of mNeonGreen (see Methods).

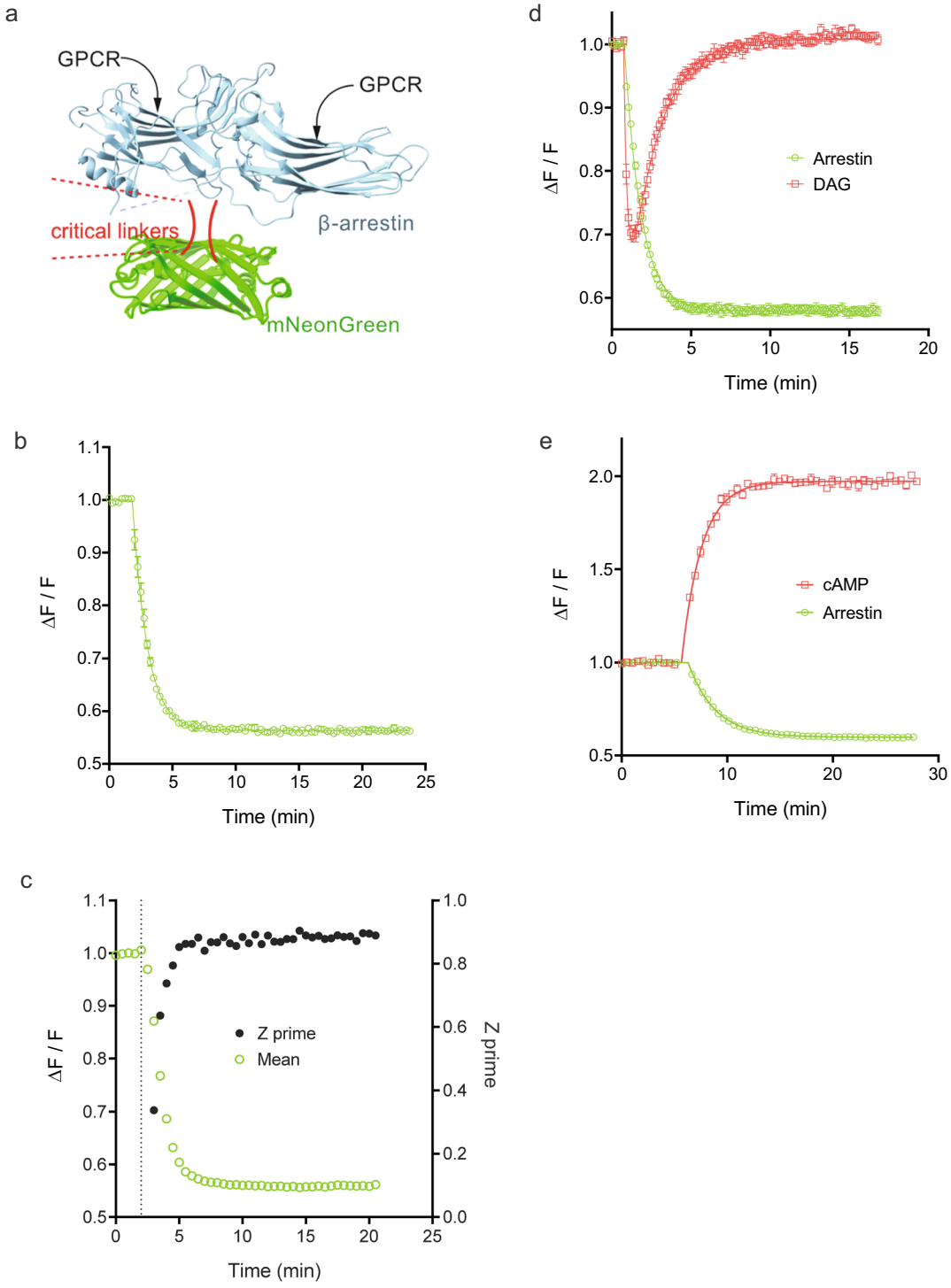

Figure 1. Characterization of a fluorescent arrestin sensor. (**a**) Schematic illustration of the arrestin biosensor. Arrestin-3 (β-arrestin2) was engineered to incorporate mNeonGreen using a screening process to identify optimal positioning and linking for generation of fluorescent signal. (**b**) Change in arrestin fluorescence on activation of the angiotensin AT_1 receptor by AngII at a concentration of 32 µM. Receptor-arrestin interaction results in a decrease of sensor fluorescence intensity. (**c**) Z′ values and mean response over the time course of AT_1 receptor-arrestin interaction stimulated by 10 µM AngII. (**d**) Multiplexing green arrestin sensor with red diacylglycerol sensor, with activation of the AT_1 receptor by 30 µM AngII. (**e**) Multiplexing with red cADD is (cAMP) sensor, with activation of the V_2 vasopressin receptor by vasopressin at 30 µM. Data were generated with the BMG CARIOstar (**b**–**d**) or Biotek Synergy Mx (**e**) plate readers. Data points are mean ± sem [n = 2 for (**b**) and n = 4 for (**d**,**e**)]. The signal was normalized to baseline; specifically it was quantified as the fluorescence after agonist addition divided by that of the baseline signal before addition (ΔF/F).

Agonist application resulted in a robust change of fluorescence intensity of the arrestin sensor, for the angiotensin AT_1 receptor (Fig. 1b) and V_2 vasopressin receptor (Fig. 1e). The signal was normalized to baseline; specifically it was quantified as the fluorescence after agonist addition divided by that of the baseline signal before addition ($\Delta F/F$). The robustness of the signal over time is a key determinant of utility for kinetic application of the sensor. Consequently, statistical analysis was conducted for the $\Delta F/F$ value at all time points measured. The angiotensin data was used for this purpose. The coefficient of variance (% CV) of the technical replicates (duplicates) is shown in Supplementary Fig. S1, for multiple concentrations of AngII spanning the effective concentration range. The % CV was less than 7% for all data points, and less than 5% in 98% of cases. This result indicates the signal is sufficiently robust to quantify the signal over the entire time course across the effective concentration range. Not surprisingly, the error was greatest when the signal was changing the most over time, i.e. on the linear part of the curve (Supplementary Fig. S1). Next we assessed the Z′ value over time to determine the ideal timeframe for a single time point measurement (Fig. 1c), the paradigm typically used for high throughput screening (HTS). Z′ is lowest on the rise phase of the time course, when the signal is changing the most over time and the magnitude of the signal is low relative to the plateau phase (Fig. 1c). At the plateau, the Z′ value was high and consistent over time. These findings indicate a time point at the plateau phase is ideal for HTS and that the signal for the AT_1 receptor is potentially robust enough for HTS.

We tested whether the arrestin sensor could be multiplexed with sensors of G-protein signaling, i.e. that the signals could be detected in the same well. The green arrestin sensor could be combined with the red diacylglycerol sensor (Fig. 1d, AT_1 receptor) and red cAMP sensor (Fig. 1e, V_2 receptor). This capability allows direct comparison of the kinetics of arrestin recruitment and G-protein signaling. For both the AT_1 receptor and V_2 receptor, the recruitment of arrestin occurs within the timeframe of the attenuation of the G-protein-mediated signal (decline of the DAG signal (Fig. 1d) and approach to plateau of cAMP concentration (Fig. 1e)). This finding is consistent with arrestin recruitment regulating (attenuating) G-protein signaling via these receptors.

Some receptors interact more transiently with arrestin than the AT_1 and V_2 receptors, for example the β_2-adrenoceptor[39]. The interaction of the arrestin sensor with the β_2-adrenoceptor was tested, in response to a maximally-stimulating concentration of isoproterenol (10 μM). The magnitude of the response was smaller (Supplementary Fig. S2); the $\Delta F/F$ value was reduced to 0.84 in this experiment, compared to a reduction to 0.56 for the AT_1 receptor in the experiment in Fig. 1b. This finding is consistent with weaker coupling of the arrestin sensor with the β_2-adrenoceptor compared with AT_1 and V_2 receptors.

Time course and concentration-dependence of arrestin recruitment by the angiotensin AT1 receptor. We next characterized the arrestin recruitment kinetics of the AT_1 receptor, examining the shape of the time course and the concentration-response characteristics. For the full agonist and endogenous ligand AngII, arrestin was initially recruited rapidly at a maximally-effective concentration (32 μM), starting within 1 minute of application (Fig. 2a). The recruitment leveled off then reached a plateau within five minutes (Fig. 2a). The plateau was stable for the remainder of the measurement period (for example, 20 min, Fig. 2a), indicating a steady-state had been obtained. By visual inspection, this profile appeared to conform to the familiar association exponential curve. The data were fit to this equation using Prism 8.0:

$$y = Plateau \times (1 - e^{-k_{obs} \cdot t})$$

where *Plateau* is the response at the asymptote (at infinite time) and k_{obs} the rate constant. Data were fit well by this equation (R^2 correlation coefficient > 0.99 in all cases). The $t_{1/2}$, calculated from k_{obs} ($t_{1/2} = 0.693/k_{obs}$) was 45 ± 3 sec at 32 μM (Supplementary Table S1). For lower, sub maximally-effective concentrations, e.g. 10 nM, the initial recruitment was slower, manifest as a shallower initial rise, and the plateau was lower (Fig. 2a). Data for lower concentrations were also fit well by the association exponential equation (Fig. 2a, $R^2 > 0.95$ in all cases). The concentration-dependence of the *Plateau* and k_{obs} parameter values is shown in Supplementary Fig. S3 - both *Plateau* and k_{obs} increased as the AngII concentration was increased.

A known partial agonist for arrestin recruitment was then tested, [sarcosine[1], Ile[4], Ile[8]]AngII (SII)[40]. Superficially, visual inspection of the plots suggests little difference between SII and AngII at the maximally-effective concentration of 32 μM (Fig. 2a,b). However, the ability to accurately quantify the kinetics of the response indicated an appreciable difference in the rate of arrestin recruitment; the $t_{1/2}$ of SII calculated from k_{obs} was 84 ± 21 sec, approximately twice that of AngII (45 sec) (Supplementary Table S1). This indicated SII recruits arrestin more slowly than AngII, providing a kinetic perspective on its partial agonist activity. By contrast, at the plateau, there was no appreciable difference between SII and AngII (compare 32 μM data in Fig. 2a,b, Supplementary Table S1). This finding indicates that if arrestin recruitment was measured at a single time point on the plateau, the difference of activity between the peptides would not have been detected; SII would have appeared to be a full agonist. Only by measuring the rate of arrestin recruitment was the partial agonist activity revealed.

Pharmacological analysis model of receptor-arrestin interaction kinetics. Applying kinetics to development of new ligands in pharmacological discovery requires the extraction of simple drug parameters from time course data. The time course of arrestin recruitment conformed to an association exponential curve for the AT_1 receptor (see above) and the V_2 receptor (Fig. 1e). A number of empirical drug parameters can be obtained from these data, such as the $t_{1/2}$, plateau, AUC, or the signal at a single time point. An alternative and biologically meaningful parameter is the initial rate of signaling, analogous to the initial rate of enzyme activity[24,25]. We recently discovered this parameter can be easily obtainable from signaling kinetic data using a kinetic pharmacological framework of GPCR signaling (Fig. 3)[25]. This approach is based on the principles of enzyme kinetic data analysis. An enzyme converts a substrate into a product (Fig. 3a). By analogy, a GPCR converts a precursor of the

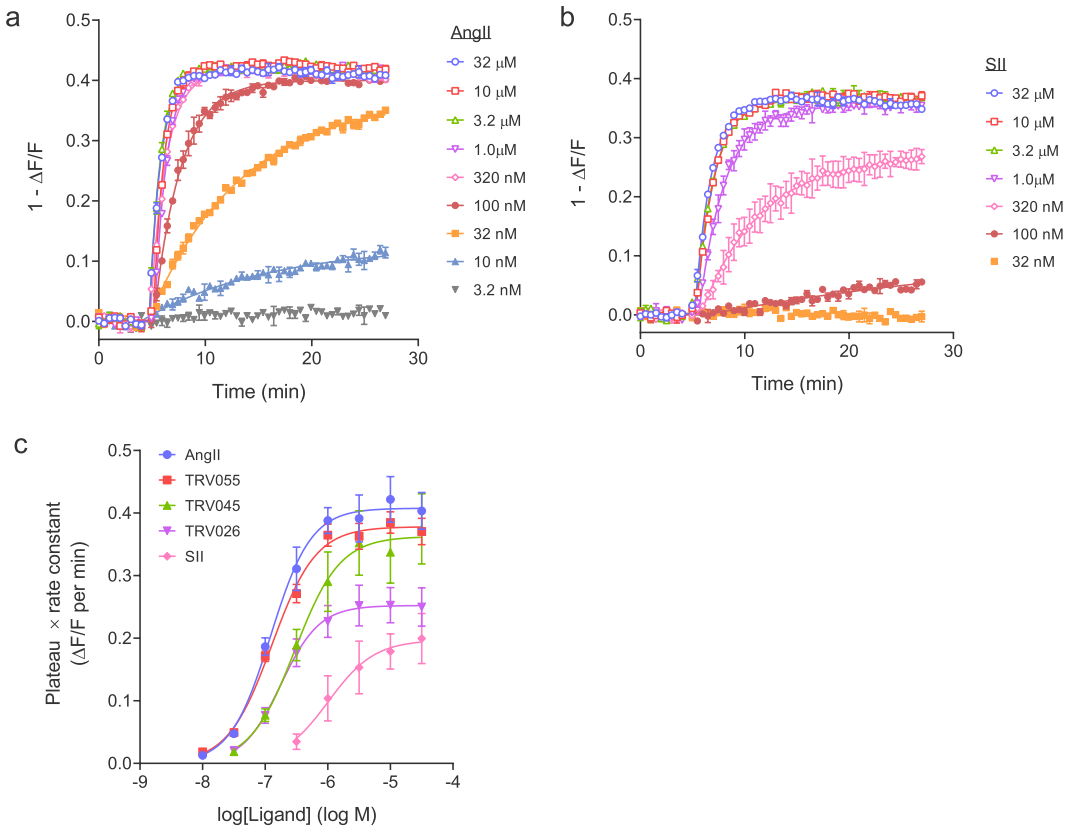

Figure 2. Dose response kinetic analysis for arrestin recruitment to the AT_1 angiotensin receptor. The time course of the arrestin sensor response was measured for a range of concentrations of AT_1 receptor agonists AngII (**a**), SII (**b**) and TRV055, TRV045 and TRV026 (Supplementary Fig. S7). Data are well fit by the association exponential equation, $y = Plateau \times (1 - e^{-k_{obs} \cdot t})$, as predicted by the kinetic model of arrestin recruitment (Appendix). From these fits it is possible to measure k_τ, the initial rate of arrestin recruitment by the agonist-bound receptor. First, the *Plateau* value is multiplied by the k_{obs} value. The resulting value is plotted against the agonist concentration, shown in panel (c). These data are then fit to a dose-response equation ("Log(agonist) vs. response–Variable slope" equation in Prism[46]). k_τ is the top of the curve, the $Plateau \times k_{obs}$ value at maximally-effective agonist concentrations. Agonist affinity for the receptor is the L_{50} of the sigmoid curve. Data are from the Biotek Synergy Mx plate reader. The signal was normalized to baseline; specifically it was quantified as the fluorescence after agonist addition divided by that of the baseline signal before addition (ΔF/F).

signal into the signal (Fig. 3b), for example, conversion of inactive G-protein to active G-protein. For enzymes, the initial rate of activity is the rate before it becomes limited by regulation mechanisms and depletion of the substrate. By analogy, the initial rate of GPCR signaling is the rate before signaling regulation mechanisms limit the signal (Fig. 3c)[25]. The canonical short-term regulation of signaling mechanisms are receptor desensitization, and degradation of the signal (e.g. hydrolysis of GTP bound to G-protein or clearance of cytoplasmic Ca^{2+}). The response can also become limited by depletion of the precursor of the signal, e.g. depletion of Ca^{2+} from intracellular stores. The initial rate is defined by the law of mass action, being a function of the interacting components and a microscopic rate constant. For enzymes the initial rate is $[E]_{TOT}[S]_{TOT}k_{CAT}$ (product of total enzyme, total substrate, and the catalytic rate constant). By analogy, for GPCR signaling, the initial rate is $E_{P(TOT)}[R]_{TOT}k_E$, where $E_{P(TOT)}$ is the total precursor, $[R]_{TOT}$ the total receptor concentration, and k_E a rate constant termed the transduction rate constant[24,25]. This is the initial rate of signaling by the ligand-bound receptor and is termed k_τ. This parameter can be easily estimated by curve fitting[25].

Here we developed a pharmacological analysis that can be applied to measure the initial rate of arrestin recruitment, the direct analogue of the initial rate of signaling described above. The mechanism of arrestin recruitment is known. Agonist-bound GPCR is phosphorylated by kinase enzymes[41,42] and the phosphorylated receptor binds arrestin[43,44]. This mechanism is represented as follows:

$$RA + N \underset{k_{-N}}{\overset{k_N}{\rightleftharpoons}} NRA$$

Arrestin (N) interacts with ligand-bound receptor (RA), governed by the rate constant k_N. (In most cases the rate-limiting step in arrestin recruitment is receptor phosphorylation so in these cases k_N is the rate constant for receptor phosphorylation). Arrestin dissociates from the ligand-receptor complex, governed by the

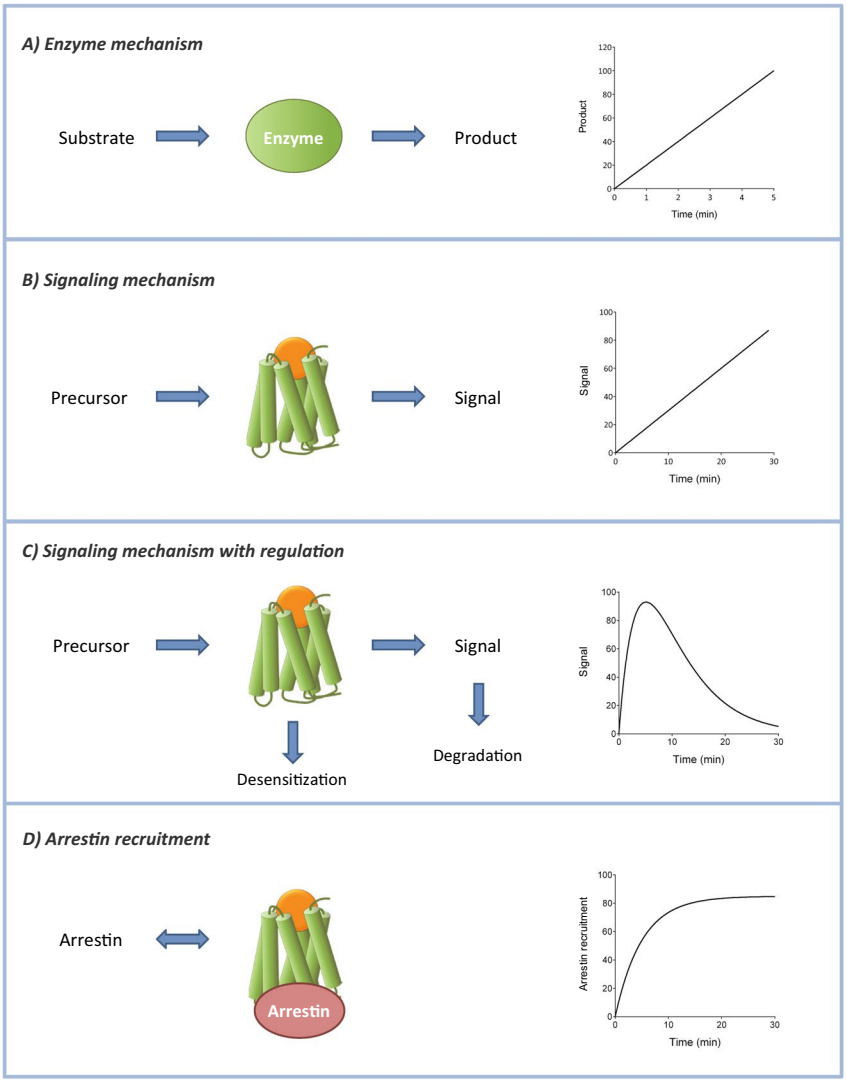

Figure 3. Receptor signaling kinetics mechanisms. A data analysis framework for quantifying the kinetics of GPCR signaling has been developed previously[24,25]. This method quantifies the initial rate of signaling (k_τ), analogous to the initial rate of enzyme activity. Here a data analysis method is introduced to quantify arrestin recruitment kinetics. (**A**) Enzyme catalysis mechanism - enzyme converts substrate to product. The time course is a straight line (under conditions of minimal substrate depletion). (**B**) GPCR signaling mechanism - agonist-bound GPCR converts a signal precursor to the signal (e.g. GDP-bound G-protein to the GTP-bound form, or sequestered Ca^{2+} to cytoplasmic Ca^{2+}). The time course is a straight line. (**C**) GPCR signaling modulated by regulation of signaling mechanisms - receptor desensitization and signal degradation. The resulting time course is a rise-and-fall curve. The shape of the time course is dependent on the number and nature of regulation mechanisms[25]. (A third regulation mechanism is depletion of signal precursor). (**D**) Arrestin recruitment - agonist-bound GPCR interacts with arrestin. The time course is an association exponential curve, as described in Results and Appendix.

arrestin-receptor dissociation rate constant k_{-N}. In the Appendix an equation was derived that describes the level of ligand-receptor-arrestin complex ($[NRA]$) over time after the addition of ligand (Eq. (3)):

$$[NRA]_t = \frac{\rho_A k_\tau}{k_{obs}}(1 - e^{-k_{obs}t})$$

where ρ_A is fractional receptor occupancy by ligand and k_{obs} the observed rate constant.

The validity of the model was assessed by comparing data simulated using the model with experimental data. In agreement with experimental data, the simulated arrestin recruitment conforms to an association exponential curve (Supplementary Fig. S4a). This is because Eq. (3) is of the form of the association exponential equation (Appendix). (It is noteworthy that once recruitment reaches a plateau then the signal remains unchanged for several minutes even though the arrestin-receptor complex interacts with internalization machinery. One possible explanation is that the interaction with the internalization machinery does not appreciably alter the fluorescence

Ligand	k_τ (NFU. min^{-1})[a]	k_τ (% AngII)	pK_A	K_A (nM)
AngII	0.41 ± 0.03	100	6.92 ± 0.06	120
TRV055	0.38 ± 0.02	93	6.90 ± 0.04	130
TRV045	0.36 ± 0.05	89	6.52 ± 0.02	300
TRV026	0.25 ± 0.03	62	6.76 ± 0.05	180
SII	0.20 ± 0.03	48	5.97 ± 0.15	1,100

Table 1. Arrestin dose response parameters from the kinetic model applied to the AT_1 angiotensin receptor. k_τ was measured from the arrestin concentration-response time course data as described in Fig. 2 and Supplementary Fig. S5. For k_τ normalized to AngII, the mean k_τ value for the ligand was divided by that for AngII. K_A was calculated from the mean pK_A value. Data are mean ± s.e.m. from three experiments, except for SII (n = 2). [a]NFU, normalized fluorescence units.

intensity of the sensor). The concentration-response was simulated (Supplementary Fig. S4a) and the resulting k_{obs} and *Plateau* value of the association exponential fit determined (Supplementary Fig. S4b,c). Increasing the agonist concentration increased *Plateau* and k_{obs}, with both effects approaching a limit at maximally-effective agonist concentrations (Supplementary Fig. S4). This profile was in agreement with the experimental concentration-response data for the AT_1 receptor (Supplementary Fig. S3). We also simulated the change of EC_{50} over time, which showed that EC_{50} decreases over time (Supplementary Fig. S4e), in agreement with experimental data (Supplementary Table S2).

k_τ for arrestin recruitment by the ligand-bound receptor is a measurable parameter in the model. This parameter is $[N]_{TOT}[R]_{TOT}k_N$, where $[N]_{TOT}$ is total arrestin concentration. It emerges that this parameter can be quantified using the *Plateau* and k_{obs} parameters from the fit to the association exponential equation (Appendix). Specifically, k_τ is equal to the *Plateau* value multiplied by the k_{obs} value at a maximally-stimulating concentration of ligand. This can be determined using either a full concentration response (Supplementary Fig. S5) or just a maximally-stimulating concentration (Supplementary Fig. S6), as described below.

Quantifying arrestin recruitment kinetics for the angiotensin AT1 receptor - concentra-tion-response. The angiotensin AT_1 receptor is a prototypical GPCR in the study of arrestin recruitment and biased signaling. The receptor for angiotensin II (AngII), the AT_1 receptor, regulates blood pressure and consequently is a target for antihypertensive drugs (the sartan antagonists)[45]. Biased ligands at the AT_1 receptor that selectively promote arrestin recruitment while blocking G-protein signaling can elicit increased cardiac performance compared with unbiased ligands, potentially beneficial for treating cardiovascular disorders[28–31].

We used the k_τ method to quantify the kinetics of arrestin recruitment of five AT_1 receptor ligands with known varying degrees of arrestin recruitment and bias. The method for quantifying k_τ is as follows (illustrated schematically in Supplementary Fig. S5). First, the time course data for the effective concentrations (10 nM–32 μM for AngII) were fit to the association exponential equation (Fig. 2a). From these fits the fitted parameter values were taken for *Plateau* and k_{obs}. These values were then multiplied together. The resulting *Plateau* x k_{obs} values were then plotted against the ligand concentration, as shown in Fig. 2c. The resulting plot was a sigmoid curve (consistent with the theoretical prediction of the model (Supplementary Fig. S4d)). The data were then fit to the sigmoid curve equation, for example the "log(agonist) vs. response–Variable slope" equation in Prism[46]. From this fit k_τ was obtained - it is the value of the asymptote. More precisely, k_τ is the *Plateau* x k_{obs} value for a maximally-effective concentration of ligand. The theoretical basis for this calculation is shown in Appendix, "Defining the initial rate of arrestin recruitment and identifying in the equations." The fitted value for k_τ for AngII was 0.41 ± 0.03 normalized fluorescence units (NFU) per min (Table 1).

We next evaluated four synthetic AT_1 receptor ligands, SII, TRV120055, TRV120045 and TRV120026[40,47]. (For clarity, the name of the last three compounds is abbreviated to TRV055, TRV045 and TRV026). These compounds were developed in SAR campaigns aiming to identify biased ligands for the AT_1 receptor. Three of these compounds, SII, TRV045 and TRV026, have been reported to be biased for arrestin recruitment over G-protein signaling. It is important to note that the compounds are not specific for arrestin recruitment – they do possess G-protein activating activity[48,49], as shown in numerous studies of SII[50–52].

Applying the kinetic analysis method to the SII data gave the *Plateau* x k_{obs} vs ligand concentration data in Fig. 2c. Fitting the sigmoid curve equation to these data gave a k_τ value of 0.20 NFU per min (Table 1). This value is approximately half that of AngII (0.41 NFU per min). This means the initial rate of arrestin recruitment by the SII-receptor complex is approximately half that of the AngII-receptor complex. Note this provides a biologically meaningful kinetic scaling of the partial agonist activity of SII for arrestin recruitment. The degree of partial agonism can be quantified conventionally, by dividing k_τ of SII by that of AngII. This gave a normalized k_τ value of 48% for SII (Table 1).

This method was applied to the remaining three ligands. In all cases the time course data conformed to the kinetic model, being well-fitted by the association exponential equation (Supplementary Fig. S7) with the *Plateau* and k_{obs} values being dependent on agonist concentration (Supplementary Fig. S3). Applying the kinetic analysis method gave the sigmoid curves in Fig. 2c and the k_τ values in Table 1. TRV055 and TRV045 are effectively full agonists for recruiting arrestin at the initial rate (k_τ 93% and 89%, respectively, of that of AngII). The efficacy of TRV026 (62%) was intermediate between that of TRV055 and SII (Fig. 2c, Table 1).

The analysis also provides an estimate of ligand affinity for the receptor, K_A. This is given by the L_{50} of the *Plateau* x k_{obs} vs concentration sigmoid curve (Appendix, Supplementary Fig. S5, L_{50} being the concentration

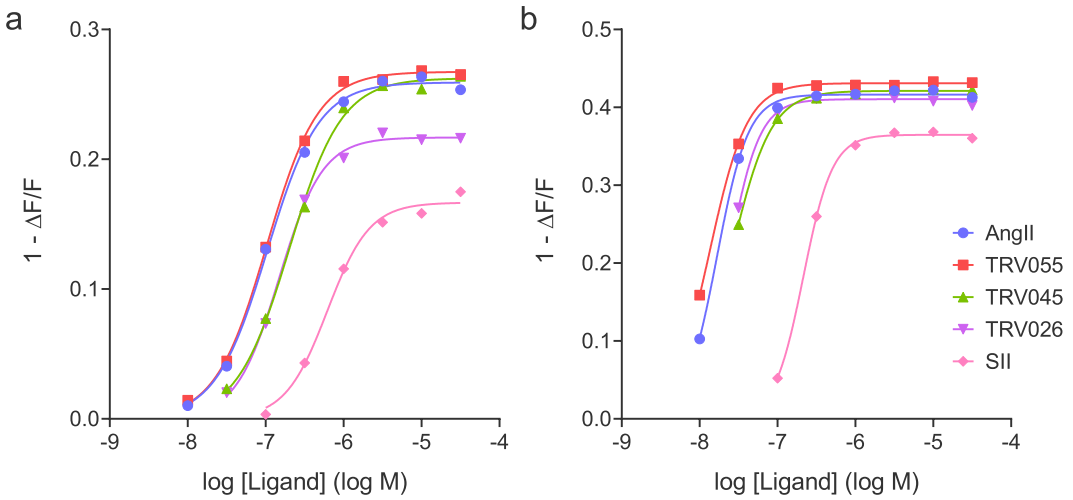

Figure 4. Single time point arrestin recruitment via the AT_1 receptor. The concentration-response for five AT_1 receptor ligands for arrestin recruitment was determined at two time points, (**a**) 1 min (representing the rise phase of the time course, Fig. 2) and (**b**) 20 min (representing the plateau) after ligand addition. This was done using the data from the representative experiments in Fig. 2 and Supplementary Fig. S7. The arrestin recruitment at the time points was calculated from the curve fits to the time course data. (Unfortunately due to slight differences in time of ligand addition in the workflow it was not possible to obtain raw data at the same specific time point for all concentrations of ligand). The concentration-response data were fit to a sigmoid dose-response equation to determine EC_{50} and E_{max}. The fitted values are given in Supplementary Table S2. Data for SII were also fit to the operational model as described in Methods, fixing the E_m value to the value of the maximal response of AngII (the "Top" value from the sigmoid curve fit, 0.259 and 0.416 normalized fluorescence units for 1 and 20 min, respectively). The τ and K_A values at 1 min were 1.8 and 1,200 nM, respectively, with corresponding values at 20 min of 7.1 and 530 nM. Note the curves from the fits to the operational model overlie those from the fits to the sigmoid curve equation.

of ligand yielding a *Plateau* x k_{obs} value half that produced by maximally-stimulating concentrations). With the exception of SII, the affinity of the ligands was similar (120–300 nM, Table 1). The affinity of SII was lower (1,100 nM, Table 1).

It is instructive to compare the pharmacology determined by the initial rate with the response at specific time points, the approach used in endpoint assays of arrestin recruitment. Fig. 4 and Supplementary Table S2 show the arrestin concentration-response curve at two different time points, 1 minute (on the rise-phase of the time course) and 20 minutes (representing the plateau phase) for the five ligands. The profile was notably different at the two time points. At 1 minute, the partial agonism of TRV045 and SII was evident from the lower maximal response (Fig. 4a). At 20 minutes, TRV045 was a full agonist and the maximal response of SII was increased close to that of the full agonists (Fig. 4b). In addition, the potency of the compounds increased over time; from 1 minute to 20 minutes, the EC_{50} decreased 3-fold for SII to 8-fold for TRV045 (Supplementary Table S2). (This reduction of EC_{50} over time is consistent with the kinetic model, see Supplementary Fig. S4e.) The pharmacological profile at 1 minute, on the rise phase, closely matched that defined by the initial rate kinetic method (Supplementary Table S2). This was anticipated, since at the 1 minute time point the response was on the linear, initial rate portion of the time course (Fig. 2a,b). The data for single time points were also fit to the operational model for the partial agonist SII, as described in Methods and the legend to Fig. 4. This analysis showed the parameter estimates were time dependent, particularly for the transducer ratio τ (1.8 at 1 min and 7.1 at 20 min) (Fig. 4). The agonist affinity estimate decreased slightly from 1 min to 20 min (from 1,200 nM to 530 nM).

Quantifying arrestin recruitment kinetics for the angiotensin AT_1 receptor - single concentration. A simplified method is feasible for measuring k_τ (see Supplementary Fig. S6). All that is required is a time course of response measurement at a single, maximally-stimulating concentration of ligand (maximally-stimulating at all time points). In Fig. 5a the data for the maximally-effective concentration of the AT_1 receptor peptides is presented (32 μM). The data were fit to the association exponential equation to determine *Plateau* and k_{obs}. k_τ was then calculated - it is the *Plateau* multiplied by k_{obs} for a maximally-stimulating concentration of ligand, as explained in the Appendix. The k_τ values for the five ligands tested are shown in Table 2 and are in good agreement with the values determined using the concentration-response method (Table 1). Comparing the multiple concentration and single concentration methods, the single-concentration method provides the benefit of a smaller experiment whereas the multiple concentration method likely provides a more accurate estimate of k_τ because it is defined as the asymptote of the curve for multiple concentrations rather than the value for a single concentration.

Application to quantifying biased agonism. Biased agonism quantification relates the capacity of a ligand to activate one pathway relative to one or more other pathways[9–12]. Numerous methods and scales have

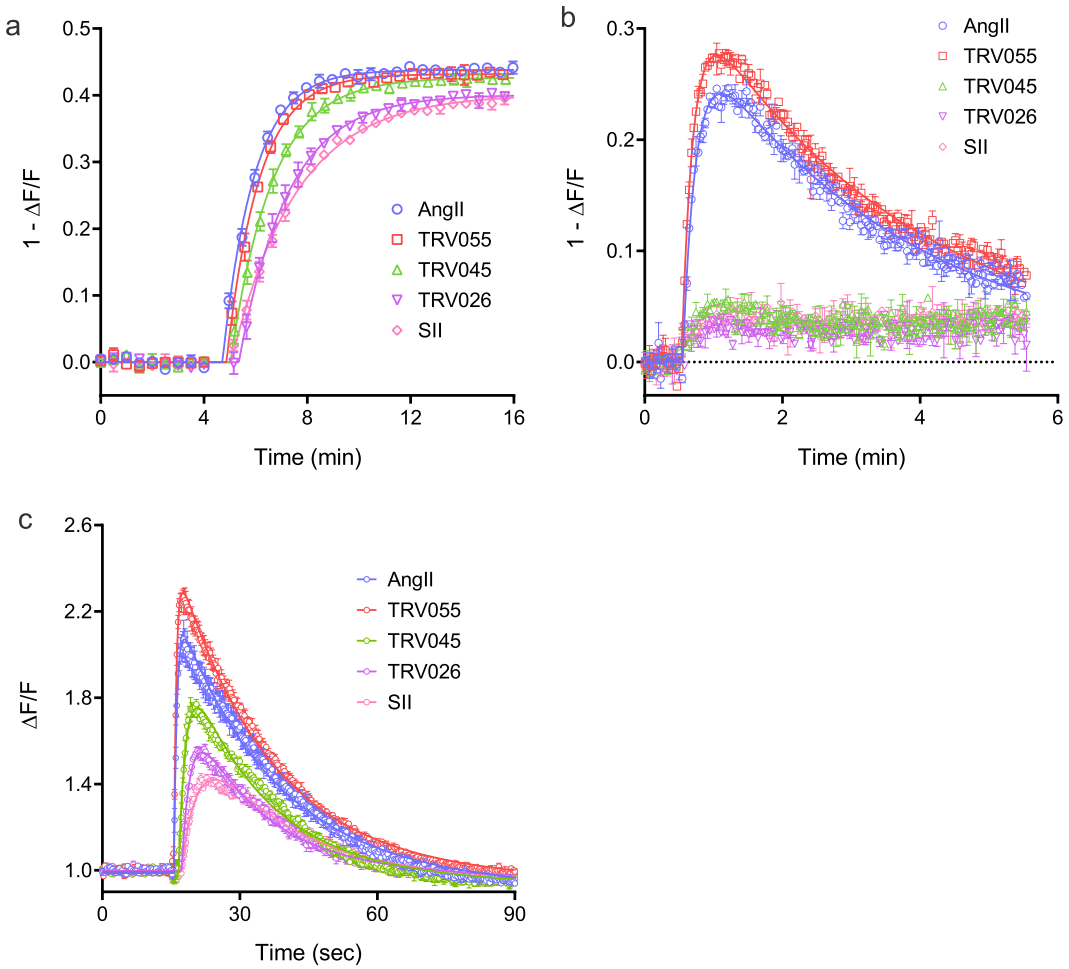

Figure 5. Kinetics of arrestin recruitment and G-protein signaling via the AT_1 angiotensin receptor, analyzed using the kinetic model. Five ligands with known signaling bias were tested for arrestin recruitment (**a**), DAG production (**b**) and Ca^{2+} mobilization (**c**). A maximally-stimulating concentration of ligand was used (32 µM), enabling k_τ to be quantified as described in Supplementary Fig. S6 for arrestin recruitment. For DAG production and Ca^{2+} mobilization k_τ was determined by fitting to the rise-and-fall exponential equation[24,25] (see Methods); the fitted value of C is equal to k_τ. The k_τ values are given in Table 2. The signal was normalized to baseline; specifically it was quantified as the fluorescence after agonist addition divided by that of the baseline signal before addition (ΔF/F). Note the signal for arrestin and DAG has been normalized to give an upward response to the downward sensor (1 − ΔF/F). All data are from the Biotek Synergy Mx plate reader.

	Arrestin		Diacylglycerol			Calcium		
Ligand	k_τ (NFU.min^{-1})[1]	k_τ (% AngII)	k_τ (NFU.min^{-1})[1]	k_τ (% AngII)	Arrestin/DAG k_τ ratio (% AngII ratio)	k_τ (NFU.min^{-1})[1]	k_τ (% AngII)	Arrestin/Ca^{2+} k_τ ratio (% AngII ratio)
AngII	0.40 ± 0.03	100	1.7 ± 0.2	100	1.00	2.2 ± 0.2	100	1.0
TRV120055	0.37 ± 0.02	92	2.1 ± 0.1	120	0.74	2.5 ± 0.2	110	0.81
TRV120045	0.38 ± 0.06	93				0.66 ± 0.02	30	3.1
TRV120026	0.25 ± 0.03	62				0.46 ± 0.08	21	3.0
SII	0.20 ± 0.04	49				0.25 ± 0.06	12	4.2

Table 2. k_τ values and ratios for AT_1 angiotensin receptor-mediated arrestin recruitment, diacylglycerol production and calcium mobilization. k_τ was measured from the time course data for a maximally-stimulating concentration of ligand (32 µM) as described in Fig. 5 and Supplementary Fig. S6. For k_τ normalized to AngII, the mean k_τ value for the ligand was divided by that for AngII. The k_τ ratio was calculated by dividing k_τ normalized to AngII for arrestin by k_τ normalized to AngII for the pathway (DAG or Ca^{2+}) Data are mean ± s.e.m. from three experiments, except for SII in arrestin recruitment (n = 2). [1] NFU, normalized fluorescence units.

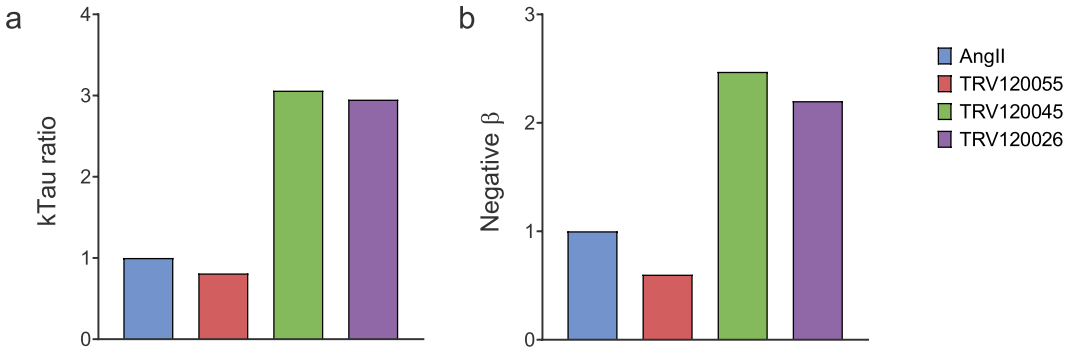

Figure 6. Comparison of k_τ bias ratio with published bias values obtained using the operational model. Bias for arrestin recruitment over Gq signaling via the AT_1 receptor is shown. The k_τ bias ratio for arrestin-3 recruitment over Ca^{2+} mobilization (**a**) was calculated as shown in Table 2. In (**b**) the bias factor was obtained using the operational model applied to data at a single time point, for arrestin-3 recruitment and inositol-1-phosphate production. Data are from Table 2 of ref. [47].

been developed and successfully applied[8,47,53–59]. One approach is to compare ligand efficacy, i.e. the capacity of the agonist-occupied receptor to generate the signal. k_τ provides such an efficacy value, being the initial rate of signal generation by the agonist-occupied receptor. Here k_τ is used to assess signaling bias of the AT_1 receptor ligands described above. These ligands have been reported to vary in their bias, with SII, TRV026 and TRV045 being arrestin biased[47–49] and TRV 055 being unbiased relative to AngII[47]. In this study, G-protein signaling and arrestin recruitment was measured using the same fluorescent biosensor assay modality, enabling near-identical conditions to be employed in comparing the pathways. The Gq pathway was quantified at the level of diacylglycerol using the Red Downward DAG sensor[21] (Fig. 5b), and, one step downstream, Ca^{2+} mobilization measured using the R-GECO sensor[22] (Fig. 5c).

The arrestin, DAG and Ca^{2+} data are shown in Fig. 5, for a maximally-stimulating concentration of the five ligands (32 μM). It is immediately obvious that curve shapes are different for the pathways - an association exponential curve defines arrestin recruitment (Fig. 5a) and a rise-and-fall curve defines DAG and Ca^{2+} signaling (Fig. 5b,c). The kinetic analysis method was designed to handle this scenario - the initial rate can be extracted from different curve shapes[24,25]. The initial rate of arrestin recruitment was quantified as described above, by multiplying the rate constant by the plateau of the association exponential fit, and the resulting k_τ values are in Table 2. For DAG and Ca^{2+}, a rise-and-fall exponential equation was applied:

$$y = \frac{C}{k_{obs1} - k_{obs2}}(e^{-k_{obs2}t} - e^{-k_{obs1}t})$$

k_τ is equal to the value of C in this equation[24,25]. The equation assumes two regulation mechanisms are in operation, corresponding to the two exponent terms. (These are most likely receptor desensitization and response degradation for DAG, and precursor depletion and response degradation for the shorter-term Ca^{2+} response[25]). The fitted k_τ values for DAG and Ca^{2+} are shown in Table 2. For DAG, no response was detectable for TRV045, TRV026 and SII. Responses to these peptides were observed for Ca^{2+}, one step downstream and so potentially more sensitive to small effects owing to signal amplification.

The next step in the bias calculation is normalization to a reference agonist. AngII was used for this purpose, being a full agonist and the endogenous ligand. The resulting normalized k_τ values are shown in Table 2. A qualitative assessment of bias can be made with these values. All ligands appreciably stimulate arrestin recruitment (by ≥49%, Table 2). By contrast, only weak activation of the Gq pathway was detected for three of the ligands (TRV045, TRV026 and SII); DAG was not detectable, and only a weak maximal effect was observed in the more amplified Ca^{2+} signal (12–30%, Table 2). This finding suggests the ligands are biased for arrestin recruitment over Gq signaling.

The final, quantitative step in the bias assessment is the bias ratio calculation. This was done by dividing the normalized k_τ value for arrestin recruitment by that for Ca^{2+}. By definition, the ratio for the reference ligand AngII was 1.0 (Table 2). Three ligands were arrestin-biased, evidenced by their arrestin/Ca^{2+} k_τ ratio being greater than 1 (3.1, 3.0 and 4.2 for TRV045, TRV026 and SII, Table 2). One ligand was unbiased, relative to AngII (TRV055, Table 2). These results are consistent with the known bias profiles of these ligands[47–49]. For example, SII is an established arrestin-biased AT_1 receptor ligand, and TRV055 is known as a balanced ligand (relative to AngII). In Fig. 6, the bias factor from the k_τ ratio was compared with the bias factor calculated previously using a validated method, the operational model approach[47]. The bias profile across the four ligands tested was similar; TRV 055 was similar to AngII, whereas TRV045 and TRV026 were arrestin-biased and the degree of bias was similar for both ligands (Fig. 6).

These results indicate bias can be calculated simply and in kinetic terms using a common data analysis framework, the k_τ method, for G-protein signaling and arrestin recruitment. The application of a common detection modality for arrestin and G-protein (the genetically-encoded sensors) also provides a unified technical platform that simplifies the interpretation of bias.

Discussion

Arrestin recruitment to GPCRs is the first step in a pathway that mediates myriad GPCR responses[26,27] that are often selectively activated over G-protein pathways by biased agonists [10,15,36,48,49]. Here we developed a method of quantifying arrestin-receptor interaction that takes into account the kinetics, i.e. the time course, of the response. We developed an improved kinetic arrestin assay. Present assays include endpoint assays, requiring a plate for every time point, or employ bioluminscent resonance energy transfer-based sensors that often require read times too long to accommodate the rapid changes of arrestin recruitment typically observed for GPCRs. A data analysis framework was developed to analyze time course data to quantify arrestin recruitment in kinetic terms, specifically the initial rate of recruitment. The resulting values can be directly compared with the initial rate of signaling through other pathways, enabling straightforward assessment of biased agonism. Application of this approach to biased agonists of the AT_1 angiotensin receptor provided bias estimates similar to literature values, suggesting the method can be applied generally to quantify biased agonism.

The arrestin sensor is a genetically-encoded arrestin protein modified to incorporate the intrinsically-fluorescent protein mNeonGreen[37,38]. The fluorescent protein is incorporated in such a way as to render the fluorescence emission conformationally-sensitive, such that interaction with the GPCR results in a decrease of fluorescence intensity. The sensor was designed to meet criteria necessary for application to drug discovery. The high quantum yield provides a large enough signal for detection in plate readers and enables short excitation times to be used, which minimizes photobleaching[21]. BacMam provides consistent receptor and biosensor expression, minimizing cell to cell and well to well variability. Importantly the BacMam delivery can adjust to optimize expression levels. The Z-score was high enough for the AT_1 and V_2 receptors for application to HTS and lead optimization. Minimal steps are required for the assay; once the cells are prepared, the only reagent addition step is the application of agonist. The absence of subsequent detection reagent additions improves workflow and likely contributes to the high Z-score. The disadvantage of the sensor for HTS is that fluorescent compounds can potentially interfere with the assay because direct fluorescence excitation-emission is employed, requiring a follow-up assay to test for compound fluorescence. This is likely less of an issue in lead optimization, by which time fluorescent molecules, usually undesirable, have been disregarded. The sensor also possesses desirable pharmacological properties that simplify the analysis and interpretation of data in lead optimization, specifically, 1) The unmodified receptor can be used, providing estimates of authentic rather than forced coupling to arrestin. 2) The detection of the interaction is at the level of the receptor interaction itself, rather than downstream (for example, activation of transcription factors or phosphorylation of extracellular signal-regulated kinase). As a result, there is no receptor reserve, simplifying interpretation of ligand efficacy for arrestin recruitment; the maximal response to ligand is equal to the efficacy of the ligand. The sensor is ideal for kinetic measurements. The short excitation time enables a short time interval between data points of the time course (e.g. 9 sec, Fig. 1d). The high reproducibility provides robust data at early time points, when the change of signal is small but the value of the data point to defining the kinetics is high (Fig. 1c, Supplementary Fig. S1). Finally, two or more pathways can be quantified using the same modality (and in the case of multiplexing, in the same cells, Fig. 1d,e), ideal for assessing biased agonism. This avoids complications arising from the use of different assay systems for the pathways being compared, for example different biological material (e.g. membranes for GTP¬S binding and cells for arrestin recruitment), different time points, buffer conditions, temperatures and so on.

A data analysis framework was required to translate the arrestin time course data into a useful pharmacological parameter. Previously we have quantified G-protein signaling kinetics using the initial rate of signaling, which we termed k_τ[24,25]. Here this concept was extended to arrestin recruitment. (This was necessary because the original mechanism described generation of a downstream signal, whereas the arrestin sensor signal reports direct receptor-effector interaction.) The resulting analysis quantifies the initial rate of arrestin recruitment, i.e. the same parameter as that used previously for G-protein signaling. k_τ is reasonably straightforward to measure from time course data, using either a full concentration-response (Fig. 2c, Supplementary Fig. S5) or at a single maximally-effective concentration (Fig. 5a, Supplementary Fig. S6). Time course data are fitted to the association exponential equation, fitted values of *Plateau* and k_{obs} obtained, then these values multiplied together. k_τ is *Plateau* x k_{obs} at a maximally-effective ligand concentration.

The k_τ parameter has certain benefits as a pharmacological parameter. First, it takes into account the kinetics of signaling, being a rate. In simple terms, k_τ is the same at all time points. This avoids the problem of time-dependence of ligand efficacy values that can occur when using a single time point assay[3,4,8]. Second, the initial rate is biologically meaningful; it describes the response generation (arrestin recruitment or G-protein signaling) by the receptor before the response becomes modulated by regulation of signaling mechanisms (e.g. dissociation of arrestin, and degradation of second messengers). For this reason k_τ is potentially more intuitive to use in interpreting and translating ligand efficacy than more abstract pharmacological parameters such as τ in the operational model. However, the k_τ method is relatively new and so not established. Currently unexplored is the impact of receptor reserve on k_τ estimates of downstream signaling. The current theoretical framework assumes k_τ incorporates receptor reserve[24] but the extent to which this is sufficient to explain experimental data remains to be determined.

This analysis was applied to biased agonism assessment using the AT_1 receptor (Fig. 5, Table 2). Bias between arrestin and Gq-mediated signaling was quantified using the k_τ method for five ligands. Bias was quantified as the ratio between the k_τ value, normalized to that of AngII, for arrestin and Ca^{2+}. The resulting bias estimates were in good agreement with those from previous studies (Fig. 6)[47], validating the method. The analysis clearly showed that the ligands described as arrestin-biased, such as SII, do possess G-protein activating activity, being partial agonists. The sensor and analysis platform provides an ideal system for measuring biased agonism. Technical differences between signaling assay readouts are minimized because the same assay conditions are employed for arrestin and G-protein signaling measurements - the only difference is the sensor introduced into the cells the day before assay. [Though not used in this study, the sensors can be multiplexed, which eliminates

assay condition differences completely (Fig. 1d,e)]. The use of the kinetic paradigm and k_τ eliminates the time dependence of biased agonism estimates that can result from the use of endpoint assays and single time point data analysis[8]. The unified data analysis framework enables arrestin and G-protein signaling to be directly compared using the same parameter (initial rate of arrestin recruitment or signal generation). The new analysis simplifies the determination of the bias factor. The current analysis methods are quite complex[8,47,53–59], involving multiple calculations and in some cases advanced curve fitting (such as simultaneous fitting of multiple ligand concentration-response curves). The calculations of the k_τ method are simple to perform, requiring a single bias calculation (the k_τ ratio) and employing basic, familiar curve fitting. Finally, the bias scale is more straightforward; the bias scales of existing methods are abstract, whereas the k_τ ratio is a more biologically meaningful parameter, being the ratio of the initial rate of the responses being compared.

In summary, in this study we describe a platform that utilizes the kinetics of response to quantify arrestin recruitment and G-protein-mediated signaling. This provides a universal analysis framework employing the initial rate of activity that simplifies quantification and interpretation of ligand activity and biased agonism. This method can be employed by drug discovery scientists to improve the identification, optimization and development of new therapeutics.

Methods

Sensor design. The design goals for a new arrestin-3 (β-arrestin2) sensor were: 1) it needed to be bright enough for detection on automated fluorescence plate readers, 2) it needed to use a single fluorescent protein so that other portions of the visible spectrum were available for other colored sensors and multiplex recordings, and 3) the change in fluorescence in response to GPCR activation has to be large enough to produce signal-to-noise ratios of >60.

Using the arrestin-3 structures as our guide, we designed a series of constructs in which the entire arrestin-3 was inserted into the middle of the seventh stave of β-sheet in the barrel of mNeonGreen, directly adjacent to the chromophore[37,38]. The goal was to convert the change in arrestin-3 shape when it binds a phosphorylated receptor into a change in the chromophore environment resulting in a change in fluorescence intensity. The first biosensors that positioned analyte binding domains in this position used a circularly permuted version of the fluorescent protein, and include the GCaMP and GECO Ca^{2+} sensors, the upward and downward DAG sensors, and the caDDis cAMP sensor[21,22]. More recently it has become clearer that if the termini of the analyte binding domain are close to one another, then the entire binding domain can be inserted into the 7th stave of the fluorescent protein without having to circularly permute the fluorescent protein[60].

The initial constructs were screened for responses on a fluorescence microscope with time lapse imaging, and drugs were added to the well by hand. HEK 293 T cells were transiently transfected with the sensor prototypes as well the AT_1 angiotensin receptor. The receptor was then activated with the addition of 30 μM AngII, and the sensor was monitored for changes in fluorescence. After identifying a functional prototype, mutagenic PCR was used to randomly mutagenize two to three amino acids at a time at the fusion junction/s, producing random libraries of thousands of mutants. These mutants were then screened in a high throughout format on a fluorescence plate reader for AT_1 receptor activation-dependent changes in fluorescence intensity.

BacMam production and titer. BacMam was produced following the methods described previously[21]. To establish BacMam titers, we quantified viral genes per mL using quantitative PCR. Samples are diluted 1:10 in Triton X-100, and then exposed to two freeze/thaw cycles of 5 minutes in a dry ice/ethanol bath and 2 minutes in a 42 °C water bath. Samples are then diluted 1:50 in TE buffer in preparation for use as a qPCR template. qPCR is performed using the SYBR Select Master Mix (Applied Biosystems, Waltham, MA) in a Rotor-Gene Q thermocycler (Qiagen, Germantown, MD). PCR primers are specific to the VSVG gene (Forward Primer 5' GCAAGCATTGGGGAGTCAGAC 3', Reverse Primer 5' CTGGCTGCAGCAAAGAGATC 3'). Viral stocks are tested monthly and are typically stable for 12 months when stored at 4 °C and protected from light. While viral genes/mL is a reliable, consistent measurement of viral concentration, the efficiency by which a viral stock successfully transduces mammalian cells varies by cell type, the promoter used to drive expression, and the means by which transduction is detected.

Molecular biology. The cDNA for the AT_1 angiotensin receptor and V_2 vasopressin receptor were obtained from the cDNA Resource Center (Bloomsburg University, Bloomsburg, PA). The cDNA encoding the arrestin-3 sensor, Red DAG sensor, R-GECO sensor, Red cADDis sensor, and the receptors were cloned into the same vector which put them under the transcriptional control of a CMV promoter.

Cell culture and viral transduction. HEK 293 T cells were cultured in Eagle's minimum essential media (EMEM) supplemented with 10% fetal bovine serum (FBS) and penicillin-streptomycin at 37 °C in 5% CO_2. For BacMam transduction, cells were resuspended in media at a density of 52,000 cells per 100 μL. 100 μL of this suspension was combined with BacMam containing the arrestin-3, Red Downward DAG, Red Upward cADDis, and/or R-GECO sensors and the indicated receptors, 2 mM sodium butyrate, and EMEM in a final volume of 150 μL. For each experiment 4.24×10^8 viral genes of arrestin virus were added to each well. For multiplex experiments, 4.79×10^8 viral genes of the Red DAG sensor or 6.18×10^8. Viral genes of the Red cADDis (cAMP) sensor were added with the arrestin sensor. For experiments with the R-GECO sensor, 8.46×10^8 viral genes were added to each well. The viruses carrying the AT_1 and V_2 receptors were added such that 2.12×10^8 and 3.04×10^8 viral genes went into each well, respectively. For the β_2-adrenoceptor experiment, 4.28×10^8 viral genes for the receptor and 2.13×10^8 viral genes of GPCR kinase 2 were added to each well. The cell/transduction mixture was then seeded into 96-well plates and incubated for ~24 hours at 37 °C in 5% CO_2. Thirty minutes prior to fluorescence

plate reader or imaging experiments, the media in each well was replaced with 150 µL of Dulbecco's phosphate buffered saline (DPBS) supplemented with Ca^{2+} (0.9 mM) and Mg^{2+} (0.5 mM).

Automated plate reader assays. Fluorescence plate reader experiments were performed on the BioTek Synergy Mx (BioTek, Winooski, VT) and BMG CLARIOstar (BMG Labtech, Cary, NC) in 96 well plates. On the Biotek Synergy Mx plate reader, green fluorescence detection was recorded using 488/20 nm excitation and 525/20 nm fluorescence emission, while red fluorescence detection was recorded using 565/20 nm excitation wavelength and 603/20 nm fluorescence emission. On the BMG CLARIOstar plate reader, green fluorescence detection was recorded using 488/14 nm excitation wavelength and 535/30 nm fluorescence emission, while red fluorescence detection was recorded using 566/18 nm excitation wavelength and 620/40 nm fluorescence emission. Drug was added manually with a multichannel pipette in a volume of 50 µL at the indicated time points. While all of the data reported here came from cells in 96 well plates, we and others have been successful using this assay in the 384 well format.

Drug compounds. Vasopressin was obtained from Cayman Chemical (Ann Arbor, MI). Angiotensin II and SII (Sar[1], Ile[4,8])-Angiotensin II)[40] were obtained from Genscript (Piscataway, NJ) and MyBioSource (San Diego, CA), respectively. Trevena peptides TRV120026, TRV120045, and TRV120055[47] were synthesized by Genscript. For clarity, the ligand names are abbreviated to TRV026, TRV045 and TRV055. All working concentration of drugs were dissolved in DPBS and added manually to the HEK 293 T cells at the indicated concentrations and time points.

Data analysis. Fluorescence data were normalized to baseline. Specifically, baseline fluorescence i.e. prior to the addition of compound, was measured over at least 5 time points and the average baseline value calculated. The fluorescence value in the well subsequent to the addition of compound or vehicle was divided by the average baseline value for that well, giving the baseline-normalized fluorescence value (Δ F/F). For fitting of the model equations, in which stimulation of signaling was analyzed, downward sensor data were first normalized to be upward (arrestin sensor data in Fig. 2a,b, Fig. 4, Fig. 5a and Supplementary Fig. S7, and DAG sensor data in Fig. 5b)). This was done by subtracting the baseline-normalized value from unity ($1 - \Delta F/F$). This approach enabled a unified presentation and analysis of stimulation of signaling data.

Curve fitting was performed using Prism 8.1 (Graphpad Software, San Diego, CA). Time course data were fit to exponential equations. The time course data included the baseline phase and the equation incorporated a parameter which represents baseline fluorescence ("*y*0" or "*Baseline*" - see below). For downward responses data were fit to the "Plateau followed by one phase decay" equation built into Prism[61]:

$$y = \text{if}(x < x0,\ y0,\ Plateau + (y0 - Plateau)e^{-K.(x-x0)})$$

where *y*0 is the baseline signal, *x*0 the time of initiation of the signal, *Plateau* is the signal at the plateau (formally the asymptote as time approaches infinity) and *K* the observed rate constant in units of $time^{-1}$. For upward responses data were fit to the "Plateau followed by one phase association" equation built into Prism[62]:

$$y = \text{if}(x < x0,\ y0,\ y0 + (Plateau - y0)(1 - e^{-K.(x-x0)}))$$

For the rise-and-fall DAG response (Fig. 5b) data were fit to a user-defined bi-exponential equation[24]:

$$y = \text{if}\left(x < x0,\ Baseline,\ Baseline + \frac{C}{K_1 - K_2}(e^{-K_2(x-x0)} - e^{-K_1(x-x0)})\right)$$

where "*Baseline*" is the baseline signal (response before addition of ligand), *C* a fitting constant, and K_1 and K_2 rate constants for the two exponential phases in units of $time^{-1}$. This is the general form of the two component signaling model[24,25]. The calcium response also conformed to a rise-and-fall curve but the baseline response drifted downwards slightly (Fig. 5c). Specifically, the plateau at late time points was slightly lower than the baseline fluorescence prior to the addition of ligand. This drift was incorporated by introducing a drift parameter into the bi-exponential equation:

$$y = \text{if}\left(x < x0,\ Baseline + Drift \times x,\ Baseline + Drift \times x0 + Drift \times (x - x0) + \frac{C}{K_1 - K_2}(e^{-K_2(x-x0)} - e^{-K_1(x-x0)})\right)$$

In all the analyses, *x*0, the time of initiation of the signal, was allowed to vary in the analysis (as opposed to being held constant) to accommodate slight differences between wells in the time of addition of ligand.

Concentration-response data were fit to a sigmoid curve equation, the "Log(agonist) vs. response–Variable slope" equation in Prism[46]:

$$y = Bottom + \frac{Top - Bottom}{1 + 10^{(\text{Log}L_{50} - x) \times HillSlope}}$$

The "*Bottom*" parameter was constrained to zero in the case of the k_τ analysis, in which the *Plateau* x k_{obs} value is plotted against the agonist concentration. (Note in the Prism formulation, L_{50} is written as EC_{50}. The EC_{50} term is not used here because it has an explicit pharmacological definition[63]).

SII concentration-response data for single time points were fit to the operational model of agonism[64], using the following equation entered as a user-defined equation in Prism:

$$y = \frac{E_m \rho_A \tau}{1 + \rho_A \tau}$$

$$\rho_A = \frac{[A]^n}{{K_A}^n + [A]^n}$$

where E_m is the maximal response of the system, τ the transducer ratio, $[A]$ the ligand concentration, $K_A$the agonist affinity (specifically the agonist equilibrium dissociation constant) and n the agonist binding slope factor. In the analysis it was assumed E_m was equal to the maximal response to AngII at the time point under study and so this value was entered as a constant as the "Top" value for AngII from the fit to the sigmoid curve equation.

Technical replicates in the data sets were considered separate points in the curve fitting analysis.

Appendix: Arrestin Recruitment Mechanism and Equations

GPCRs interact with arrestin and this interaction can be detected directly using optical biosensors. In this study the biosensor was a conformationally-sensitive mNeonGreen-tagged arrestin in which the optical properties changed upon binding to the GPCR. The interaction can be described as a straightforward bimolecular interaction between the two proteins, as indicated in the following scheme:

$$RA + N \underset{k_{-N}}{\overset{k_N}{\rightleftharpoons}} NRA$$

N is arrestin, R is receptor and A is the ligand. RA is receptor-ligand complex and NRA the ternary complex of arrestin, receptor and ligand. k_N is the association rate constant for receptor-arrestin association. The value of this parameter is most likely determined by the rate of receptor phosphorylation since this is the rate-limiting step in receptor-arrestin association. k_{-N} is the arrestin-receptor dissociation rate constant. K_A is the affinity constant for ligand binding to the receptor (more precisely, the equilibrium dissociation constant). It is assumed that ligand binding is at equilibrium with the receptor, that the unbound receptor (R) does not bind arrestin, and that ligand dissociation from the ternary complex NRA is much slower than that from the binary complex RA.

Equations defining the change of signal (arrestin-receptor complex, NRA) over time were derived. From these equations the initial rate of arrestin recruitment by the ligand-bound receptor (k_τ) emerged as a readily-measurable parameter. Two scenarios regarding stoichiometry were formularized – receptor excess over arrestin (the most likely scenario in this study) and arrestin excess over receptor. Both formulations yield k_τ, and k_τ is measured in the same way for both scenarios. Here the equations for arrestin-receptor complex are solved for the two scenarios, then the identity of the initial rate in the equations demonstrated, and finally the method for measuring the initial rate (k_τ) presented.

Receptor excess over arrestin. In this scenario it is assumed receptor is in sufficient excess over arrestin that the arrestin-receptor complex does not appreciably deplete the concentration of receptor. The differential equation defining the change of receptor-arrestin complex over time is,

$$\frac{d[NRA]}{dt} = [RA][N]k_N - [NRA]k_{-N}$$

In this case the units of k_N are receptor units^{-1}.min^{-1}. $[RA]$ can be expressed as a function of the total receptor concentration, as follows. First, since we assume $[NRA]$ does not appreciably deplete the total receptor concentration, the conservation of mass equation for the receptor can be written as,

$$[R]_{TOT} \approx [R] + [RA]$$

Next, $[R]$ is substituted in this equation. Since ligand-receptor binding is at equilibrium, $[R]$ can be defined as,

$$[R] = \frac{[RA]K_A}{[A]}$$

Substituting and rearranging gives the desired expression for $[RA]$:

$$[RA] = \rho_A[R]_{TOT}$$

where ρ_A is fractional occupancy of receptor by A, defined by,

$$\rho_A = \frac{[A]}{K_A + [A]}$$

Substituting into the differential equation for $[NRA]$ gives,

$$\frac{d[NRA]}{dt} = \rho_A[N][R]_{TOT}k_N - [NRA]k_{-N}$$

Next the $[N]$ term is substituted with an expression for the total concentration of arrestin. In this scenario, the conservation of mass equation for arrestin is:

$$[N]_{TOT} = [N] + [NRA]$$

Solving for $[N]$ and substituting into the differential equation gives,

$$\frac{d[NRA]}{dt} = \rho_A[R]_{TOT}[N]_{TOT}k_N - [NRA]k_{obs1}$$

where,

$$k_{obs1} = \rho_A[R]_{TOT}k_N + k_{-N}$$

Integrating gives the desired equation defining $[NRA]$ over time, Eq. (1):

$$[NRA]_t = \frac{\rho_A[N]_{TOT}[R]_{TOT}k_N}{k_{obs1}}(1 - e^{-k_{obs1}t}) \quad (1)$$

Arrestin excess over receptor. In this scenario it is assumed arrestin is in sufficient excess over receptor that the arrestin-receptor complex does not appreciably deplete the concentration of arrestin. The differential equation defining the change of receptor-arrestin complex over time is the same as for the receptor excess assumption given above:

$$\frac{d[NRA]}{dt} = [RA][N]k_N - [NRA]k_{-N}$$

In this case the units of k_N are arrestin units^{-1}.min^{-1}. Since N is in excess over R, the free concentration of N is approximately equal to the total concentration of N, $[N]_{TOT}$. Consequently, the differential equation can be written as,

$$\frac{d[NRA]}{dt} = [N]_{TOT}[RA]k_N - [NRA]k_{-N}$$

Next, $[RA]$ in this equation can be expressed as a function of $[R]_{TOT}$. The conservation of mass equation is,

$$[R]_{TOT} = [R] + [RA] + [NRA]$$

This equation can be rearranged and solved for $[RA]$, utilizing the expression $[R] = [RA]K_A/[A]$:

$$[RA] = \rho_A[R]_{TOT} - \rho_A[NRA]$$

Substituting into the differential equation and rearranging gives,

$$\frac{d[NRA]}{dt} = \rho_A[R]_{TOT}[N]_{TOT}k_N - [NRA]k_{obs2}$$

where,

$$k_{obs2} = \rho_A[N]_{TOT}k_N + k_{-N}$$

Integrating gives the desired equation defining $[NRA]$ over time, Eq. (2):

$$[NRA]_t = \frac{\rho_A[N]_{TOT}[R]_{TOT}k_N}{k_{obs2}}(1 - e^{-k_{obs2}t}) \quad (2)$$

Defining the initial rate of arrestin recruitment and identifying it in the equations. The initial rate of arrestin interaction with the receptor is that before depletion of arrestin or receptor by formation of the *NRA* ternary complex, and before breakdown of the complex. This rate is defined as,

$$Initial\ rate = [N]_{TOT}[R]_{TOT}k_N$$

This parameter is a direct analogue of the initial rate of signaling in the kinetic signaling model, the equation for which is,

$$Initial\ rate = E_{P(TOT)}[R]_{TOT}k_E$$

where $E_{P(TOT)}$ is total concentration of precursor and k_E the response generation rate constant. In order to standardize the nomenclature between arrestin recruitment and the signaling models k_τ is used as the term for the initial rate of arrestin recruitment as well as that for signaling:

$$k_\tau = [N]_{TOT}[R]_{TOT}k_N$$

It is evident by visual inspection that this term, $[N]_{TOT}[R]_{TOT}k_N$ is present in the numerator of the equations for arrestin recruitment over time, Eqs. (1) and (2), reproduced here for convenience:

$$[NRA]_t = \frac{\rho_A[N]_{TOT}[R]_{TOT}k_N}{k_{obs1}}(1 - e^{-k_{obs1}t})$$

$$[NRA]_t = \frac{\rho_A[N]_{TOT}[R]_{TOT}k_N}{k_{obs2}}(1 - e^{-k_{obs2}t})$$

Substituting k_τ for $[N]_{TOT}[R]_{TOT}k_N$ gives the equation used to analyze the time course data, Eq. (3):

$$[NRA]_t = \frac{\rho_A k_\tau}{k_{obs}}(1 - e^{-k_{obs}t}) \quad (3)$$

where,

$$k_{obs} = k_{obs1,2}$$

Estimating the initial rate by curve fitting. Here it is shown that k_τ can be measured by combining parameters from a familiar curve fitting procedure, either from a concentration-response experiment or from an experiment employing a saturating concentration of ligand (Supplementary Figs. S5 and S6, respectively). The equations for both the receptor and arrestin excess assumptions (Eqs. (1) and (2), respectively) take the form of the familiar exponential association equation:

$$y_t = Plateau \times (1 - e^{-k_{obs} \cdot t})$$

where *Plateau* is the asymptote, the value of y as time approaches infinity, and k_{obs} the observed rate constant. (This is the "One phase association" equation in GraphPad Prism[65]). By comparing with Eqs. (1) and (2), it can be seen that the parameters are defined as,

$$Plateau = \frac{\rho_A k_\tau}{k_{obs}}$$

Combining these parameters, by multiplying them together, yields k_τ multiplied by ρ_A (the fractional receptor occupancy by ligand):

$$Plateau \times k_{obs} = \rho_A k_\tau$$

Note that this expression is the same regardless of the excess scenario. It is instructive now to expand the ρ_A term:

$$Plateau \times k_{obs} = \frac{[A]}{[A] + K_A}k_\tau$$

When the ligand concentration is maximally effective for recruiting arrestin, we assume [A] is in large excess over K_A. Under this condition, the equation reduces to,

$$[Plateau \times k_{obs}]_{[A] \gg K_A} = k_\tau$$

This means that k_τ for arrestin recruitment can be measured by multiplying the plateau by the rate constant for a maximally effective concentration of ligand. This can be done either using a single, maximally stimulating concentration (Supplementary Fig. S6, Fig. 5a) or by plotting the $Plateau \times k_{obs}$ vs [A] (Supplementary Fig. S5, Fig. 2c). In the latter method, the data are analyzed using a sigmoid dose-response equation and in this case k_τ is the fitted maximum $Plateau \times k_{obs}$ value of the curve and K_A is the $[A]_{50}$ concentration, i.e. the value of [A] giving 50% of the maximal $Plateau \times k_{obs}$ value.

Global analysis of time course data for multiple agonist concentrations. An alternative method for analyzing the data is global fitting of the time course data for multiple concentrations of agonist simultaneously. This can be done by fitting data globally to Eq. (3). This requires handling of the k_{obs} term since it is dependent on the concentration of ligand. The definition of k_{obs} is dependent on whether receptor or arrestin are in excess, the equation for which is, respectively,

$$k_{obs1} = \rho_A[R]_{TOT}k_N + k_{-N}$$

$$k_{obs2} = \rho_A[N]_{TOT}k_N + k_{-N}$$

These equations reduce to a common form:

$$k_{obs1,2} = \rho_A C + k_{-N}$$

where C is a fitting constant, defining $[R]_{TOT}k_N$ if receptor is in excess and $[N]_{TOT}k_N$ if arrestin is in excess.

It is also useful to introduce a slope term (n) to accommodate experimental variability in the precision of serial dilution of the agonist, or biological processes that can deviate the agonist concentration range in the vicinity of the receptor from the concentration range added to the assay. This is done by raising the agonist concentration and agonist affinity terms to the power of the slope factor.

The resulting equation for globally analyzing the data is Eq. (4),

$$[NRA]_t = \frac{\rho_{A,n}k_\tau}{\rho_{A,n}C + k_{-N}}\left(1 - e^{-\left(\rho_{A,n}C + k_{-N}\right)t}\right)$$

where,

$$\rho_{A,n} = \frac{[A]^n}{K_A{}^n + [A]^n} \tag{4}$$

Assessing whether receptor or arrestin is in excess. In principal the component that is in excess can be determined by varying the level of receptor or arrestin and measuring the observed rate constant, k_{obs}. The rate constant value is dependent on receptor concentration if receptor is in excess and arrestin concentration if arrestin is in excess. This is because $k_{obs}$is defined as $\rho_A[R]_{TOT}k_N + k_{-N}$ when receptor is in excess and $\rho_A[N]_{TOT}k_N + k_{-N}$ when arrestin is in excess.

Received: 10 September 2019; Accepted: 20 December 2019;
Published online: 04 February 2020

References

1. Hothersall, J. D., Brown, A. J., Dale, I. & Rawlins, P. Can residence time offer a useful strategy to target agonist drugs for sustained GPCR responses? *Drug. Discov. Today* **21**, 90–96, https://doi.org/10.1016/j.drudis.2015.07.015 (2016).
2. Grundmann, M. & Kostenis, E. Temporal Bias: Time-Encoded Dynamic GPCR Signaling. *Trends Pharmacol. Sci.* **38**, 1110–1124, https://doi.org/10.1016/j.tips.2017.09.004 (2017).
3. Lane, J. R., May, L. T., Parton, R. G., Sexton, P. M. & Christopoulos, A. A kinetic view of GPCR allostery and biased agonism. *Nat. Chem. Biol.* **13**, 929–937, https://doi.org/10.1038/nchembio.2431 (2017).
4. Ferrandon, S. *et al.* Sustained cyclic AMP production by parathyroid hormone receptor endocytosis. *Nat. Chem. Biol.* **5**, 734–742, https://doi.org/10.1038/nchembio.206 (2009).
5. Tay, D., Cremers, S. & Bilezikian, J. P. Optimal dosing and delivery of parathyroid hormone and its analogues for osteoporosis and hypoparathyroidism - translating the pharmacology. *Br. J. Clin. Pharmacol.* **84**, 252–267, https://doi.org/10.1111/bcp.13455 (2018).
6. Miller, P. D. *et al.* Effect of Abaloparatide vs Placebo on New Vertebral Fractures in Postmenopausal Women With Osteoporosis: A Randomized Clinical Trial. *JAMA* **316**, 722–733, https://doi.org/10.1001/jama.2016.11136 (2016).
7. Mullershausen, F. *et al.* Persistent signaling induced by FTY720-phosphate is mediated by internalized S1P1 receptors. *Nat. Chem. Biol.* **5**, 428–434, https://doi.org/10.1038/nchembio.173 (2009).
8. Klein Herenbrink, C. *et al.* The role of kinetic context in apparent biased agonism at GPCRs. *Nat. Commun.* **7**, 10842, https://doi.org/10.1038/ncomms10842 (2016).
9. Kenakin, T. Biased Receptor Signaling in Drug Discovery. *Pharmacol. Rev.* **71**, 267–315, https://doi.org/10.1124/pr.118.016790 (2019).
10. Whalen, E. J., Rajagopal, S. & Lefkowitz, R. J. Therapeutic potential of beta-arrestin- and G protein-biased agonists. *Trends Mol. Med.* **17**, 126–139, https://doi.org/10.1016/j.molmed.2010.11.004 (2011).
11. Violin, J. D., Crombie, A. L., Soergel, D. G. & Lark, M. W. Biased ligands at G-protein-coupled receptors: promise and progress. *Trends Pharmacol. Sci.* **35**, 308–316, https://doi.org/10.1016/j.tips.2014.04.007 (2014).
12. Kenakin, T. & Christopoulos, A. Signalling bias in new drug discovery: detection, quantification and therapeutic impact. *Nat. Rev. Drug. Discov.* **12**, 205–216, https://doi.org/10.1038/nrd3954 (2013).
13. Allen, J. A. *et al.* Discovery of beta-arrestin-biased dopamine D2 ligands for probing signal transduction pathways essential for antipsychotic efficacy. *Proc. Natl Acad. Sci. USA* **108**, 18488–18493, https://doi.org/10.1073/pnas.1104807108 (2011).
14. Chen, X. *et al.* Discovery of G Protein-Biased D2 Dopamine Receptor Partial Agonists. *J. Med. Chem.* **59**, 10601–10618, https://doi.org/10.1021/acs.jmedchem.6b01208 (2016).
15. Chen, X. *et al.* Structure-functional selectivity relationship studies of beta-arrestin-biased dopamine D(2) receptor agonists. *J. Med. Chem.* **55**, 7141–7153, https://doi.org/10.1021/jm300603y (2012).
16. Klewe, I. V. *et al.* Recruitment of beta-arrestin2 to the dopamine D2 receptor: insights into anti-psychotic and anti-parkinsonian drug receptor signaling. *Neuropharmacol.* **54**, 1215–1222, https://doi.org/10.1016/j.neuropharm.2008.03.015 (2008).
17. Masri, B. *et al.* Antagonism of dopamine D2 receptor/beta-arrestin 2 interaction is a common property of clinically effective antipsychotics. *Proc. Natl Acad. Sci. USA* **105**, 13656–13661, https://doi.org/10.1073/pnas.0803522105 (2008).
18. Lohse, M. J., Nuber, S. & Hoffmann, C. Fluorescence/bioluminescence resonance energy transfer techniques to study G-protein-coupled receptor activation and signaling. *Pharmacol. Rev.* **64**, 299–336, https://doi.org/10.1124/pr.110.004309 (2012).
19. Marullo, S. & Bouvier, M. Resonance energy transfer approaches in molecular pharmacology and beyond. *Trends Pharmacol. Sci.* **28**, 362–365, https://doi.org/10.1016/j.tips.2007.06.007 (2007).
20. Halls, M. L. & Canals, M. Genetically Encoded FRET Biosensors to Illuminate Compartmentalised GPCR Signalling. *Trends Pharmacol. Sci.* **39**, 148–157, https://doi.org/10.1016/j.tips.2017.09.005 (2018).
21. Tewson, P. H., Martinka, S., Shaner, N. C., Hughes, T. E. & Quinn, A. M. New DAG and cAMP Sensors Optimized for Live-Cell Assays in Automated Laboratories. *J. Biomol. Screen.* **21**, 298–305, https://doi.org/10.1177/1087057115618608 (2016).
22. Zhao, Y. *et al.* An expanded palette of genetically encoded Ca(2)(+) indicators. *Sci.* **333**, 1888–1891, https://doi.org/10.1126/science.1208592 (2011).

23. Kenakin, T. Quantifying biological activity in chemical terms: a pharmacology primer to describe drug effect. *ACS Chem. Biol.* **4**, 249–260, https://doi.org/10.1021/cb800299s (2009).
24. Hoare, S. R. J., Pierre, N., Moya, A. G. & Larson, B. Kinetic operational models of agonism for G-protein-coupled receptors. *J. Theor. Biol.* **446**, 168–204, https://doi.org/10.1016/j.jtbi.2018.02.014 (2018).
25. Hoare, S. R. J., Tewson, P. H., Quinn, A. M., Hughes, T. E. & Bridge, L. J. Analyzing kinetic signaling data for G-protein-coupled receptors. *BiorXiv* https://www.biorxiv.org/content/10.1101/2020.01.20.913319v1 (2019).
26. Peterson, Y. K. & Luttrell, L. M. The Diverse Roles of Arrestin Scaffolds in G Protein-Coupled Receptor Signaling. *Pharmacol. Rev.* **69**, 256–297, https://doi.org/10.1124/pr.116.013367 (2017).
27. Schmid, C. L. & Bohn, L. M. Physiological and pharmacological implications of beta-arrestin regulation. *Pharmacol. Ther.* **121**, 285–293, https://doi.org/10.1016/j.pharmthera.2008.11.005 (2009).
28. Violin, J. D. *et al*. Selectively engaging beta-arrestins at the angiotensin II type 1 receptor reduces blood pressure and increases cardiac performance. *J. Pharmacol. Exp. Ther.* **335**, 572–579, https://doi.org/10.1124/jpet.110.173005 (2010).
29. Boerrigter, G. *et al*. Cardiorenal actions of TRV120027, a novel ss-arrestin-biased ligand at the angiotensin II type I receptor, in healthy and heart failure canines: a novel therapeutic strategy for acute heart failure. *Circ. Heart Fail.* **4**, 770–778, https://doi.org/10.1161/CIRCHEARTFAILURE.111.962571 (2011).
30. Boerrigter, G., Soergel, D. G., Violin, J. D., Lark, M. W. & Burnett, J. C. Jr. TRV120027, a novel beta-arrestin biased ligand at the angiotensin II type I receptor, unloads the heart and maintains renal function when added to furosemide in experimental heart failure. *Circ. Heart Fail.* **5**, 627–634, https://doi.org/10.1161/CIRCHEARTFAILURE.112.969220 (2012).
31. Ryba, D. M. *et al*. Long-Term Biased beta-Arrestin Signaling Improves Cardiac Structure and Function in Dilated Cardiomyopathy. *Circulation* **135**, 1056–1070, https://doi.org/10.1161/CIRCULATIONAHA.116.024482 (2017).
32. Bohn, L. M., Gainetdinov, R. R., Lin, F. T., Lefkowitz, R. J. & Caron, M. G. Mu-opioid receptor desensitization by beta-arrestin-2 determines morphine tolerance but not dependence. *Nat.* **408**, 720–723, https://doi.org/10.1038/35047086 (2000).
33. Bohn, L. M. *et al*. Enhanced rewarding properties of morphine, but not cocaine, in beta(arrestin)-2 knock-out mice. *J. Neurosci.* **23**, 10265–10273 (2003).
34. Raehal, K. M., Walker, J. K. & Bohn, L. M. Morphine side effects in beta-arrestin 2 knockout mice. *J. Pharmacol. Exp. Ther.* **314**, 1195–1201, https://doi.org/10.1124/jpet.105.087254 (2005).
35. Bu, H., Liu, X., Tian, X., Yang, H. & Gao, F. Enhancement of morphine analgesia and prevention of morphine tolerance by downregulation of beta-arrestin 2 with antigene RNAs in mice. *Int. J. Neurosci.* **125**, 56–65, https://doi.org/10.3109/00207454.2014.896913 (2015).
36. Violin, J. D. & Lefkowitz, R. J. Beta-arrestin-biased ligands at seven-transmembrane receptors. *Trends Pharmacol. Sci.* **28**, 416–422, https://doi.org/10.1016/j.tips.2007.06.006 (2007).
37. Clavel, D. *et al*. Structural analysis of the bright monomeric yellow-green fluorescent protein mNeonGreen obtained by directed evolution. *Acta Crystallogr. D. Struct. Biol.* **72**, 1298–1307, https://doi.org/10.1107/S2059798316018623 (2016).
38. Shaner, N. C. *et al*. A bright monomeric green fluorescent protein derived from Branchiostoma lanceolatum. *Nat. Methods* **10**, 407–409, https://doi.org/10.1038/nmeth.2413 (2013).
39. Moore, C. A., Milano, S. K. & Benovic, J. L. Regulation of receptor trafficking by GRKs and arrestins. *Annu. Rev. Physiol.* **69**, 451–482, https://doi.org/10.1146/annurev.physiol.69.022405.154712 (2007).
40. Holloway, A. C. *et al*. Side-chain substitutions within angiotensin II reveal different requirements for signaling, internalization, and phosphorylation of type 1A angiotensin receptors. *Mol. Pharmacol.* **61**, 768–777, https://doi.org/10.1124/mol.61.4.768 (2002).
41. Inglese, J., Freedman, N. J., Koch, W. J. & Lefkowitz, R. J. Structure and mechanism of the G protein-coupled receptor kinases. *J. Biol. Chem.* **268**, 23735–23738 (1993).
42. Stadel, J. M. *et al*. Catecholamine-induced desensitization of turkey erythrocyte adenylate cyclase is associated with phosphorylation of the beta-adrenergic receptor. *Proc. Natl Acad. Sci. USA* **80**, 3173–3177 (1983).
43. Krupnick, J. G. & Benovic, J. L. The role of receptor kinases and arrestins in G protein-coupled receptor regulation. *Annu. Rev. Pharmacol. Toxicol.* **38**, 289–319, https://doi.org/10.1146/annurev.pharmtox.38.1.289 (1998).
44. Lohse, M. J., Benovic, J. L., Codina, J., Caron, M. G. & Lefkowitz, R. J. Beta-Arrestin: a protein that regulates beta-adrenergic receptor function. *Sci.* **248**, 1547–1550 (1990).
45. Alexander, W. *et al*. *Angiotensin receptors: AT1 receptor*. www.guidetopharmacology.org/GRAC/ObjectDisplayForward?objectId=34.
46. Motulsky, H. J. *Equation: log(agonist) vs. response–Variable slope*. www.graphpad.com/guides/prism/8/curve-fitting/index.htm?reg_dr_stim_variable.htm, (2019).
47. Rajagopal, S. *et al*. Quantifying ligand bias at seven-transmembrane receptors. *Mol. Pharmacol.* **80**, 367–377, https://doi.org/10.1124/mol.111.072801 (2011).
48. Namkung, Y. *et al*. Functional selectivity profiling of the angiotensin II type 1 receptor using pathway-wide BRET signaling sensors. *Sci Signal* **11**, doi:10.1126/scisignal.aat1631 (2018).
49. Wei, H. *et al*. Independent beta-arrestin 2 and G protein-mediated pathways for angiotensin II activation of extracellular signal-regulated kinases 1 and 2. *Proc. Natl Acad. Sci. USA* **100**, 10782–10787, https://doi.org/10.1073/pnas.1834556100 (2003).
50. Sauliere, A. *et al*. Deciphering biased-agonism complexity reveals a new active AT1 receptor entity. *Nat. Chem. Biol.* **8**, 622–630, https://doi.org/10.1038/nchembio.961 (2012).
51. Grundmann, M. *et al*. Lack of beta-arrestin signaling in the absence of active G proteins. *Nat. Commun.* **9**, 341, https://doi.org/10.1038/s41467-017-02661-3 (2018).
52. Strachan, R. T. *et al*. Divergent transducer-specific molecular efficacies generate biased agonism at a G protein-coupled receptor (GPCR). *J. Biol. Chem.* **289**, 14211–14224, https://doi.org/10.1074/jbc.M114.548131 (2014).
53. Schmid, C. L. *et al*. Bias Factor and Therapeutic Window Correlate to Predict Safer Opioid Analgesics. *Cell* **171**, 1165–1175 e1113, https://doi.org/10.1016/j.cell.2017.10.035 (2017).
54. Ehlert, F. J. On the analysis of ligand-directed signaling at G protein-coupled receptors. *Naunyn Schmiedebergs Arch. Pharmacol.* **377**, 549–577, https://doi.org/10.1007/s00210-008-0260-4 (2008).
55. Hall, D. A. & Giraldo, J. A method for the quantification of biased signalling at constitutively active receptors. *Br. J. Pharmacol.* **175**, 2046–2062, https://doi.org/10.1111/bph.14190 (2018).
56. Gregory, K. J., Hall, N. E., Tobin, A. B., Sexton, P. M. & Christopoulos, A. Identification of orthosteric and allosteric site mutations in M2 muscarinic acetylcholine receptors that contribute to ligand-selective signaling bias. *J. Biol. Chem.* **285**, 7459–7474, https://doi.org/10.1074/jbc.M109.094011 (2010).
57. Evans, B. A. *et al*. Quantification of functional selectivity at the human alpha(1A)-adrenoceptor. *Mol. Pharmacol.* **79**, 298–307, https://doi.org/10.1124/mol.110.067454 (2011).
58. McPherson, J. *et al*. mu-opioid receptors: correlation of agonist efficacy for signalling with ability to activate internalization. *Mol. Pharmacol.* **78**, 756–766, https://doi.org/10.1124/mol.110.066613 (2010).
59. Kenakin, T., Watson, C., Muniz-Medina, V., Christopoulos, A. & Novick, S. A simple method for quantifying functional selectivity and agonist bias. *ACS Chem. Neurosci.* **3**, 193–203, https://doi.org/10.1021/cn200111m (2012).
60. Odaka, H., Arai, S., Inoue, T. & Kitaguchi, T. Genetically-encoded yellow fluorescent cAMP indicator with an expanded dynamic range for dual-color imaging. *PLoS One* **9**, e100252, https://doi.org/10.1371/journal.pone.0100252 (2014).
61. Motulsky, H. J. *Equation: Plateau followed by one phase decay*. www.graphpad.com/guides/prism/8/curve-fitting/reg_exponential_decay_plateau.htm?q=decay+plateau, (2019).

62. Motulsky, H. J. *How to: Plateau followed by one phase association*. www.graphpad.com/guides/prism/8/curve-fitting/reg_exponential_plateau_then_association.htm?q=association (2019).
63. Neubig, R. R., Spedding, M., Kenakin, T. & Christopoulos, A. International Union of Pharmacology Committee on Receptor Nomenclature and Drug Classification. XXXVIII. Update on terms and symbols in quantitative pharmacology. *Pharmacol. Rev.* **55**, 597–606, https://doi.org/10.1124/pr.55.4.4 (2003).
64. Black, J. W. & Leff, P. Operational models of pharmacological agonism. *Proc. R. Soc. Lond. B Biol. Sci.* **220**, 141–162 (1983).
65. Motulsky, H. J. *Equation: One phase association*. www.graphpad.com/guides/prism/8/curve-fitting/index.htm?reg_exponential_association.htm (2019).

Acknowledgements
Research reported in this publication was supported by National Institute of General Medical Sciences, National Institutes of Health under award number R44GM125390 and National Institute of Neurologic Disorders and Stroke, National Institutes of Health R44NS082222. This content is solely the responsibility of the authors and does not necessarily represent the official views of the National Institutes of Health.

Author contributions
S.R.J.H. designed the data analysis framework, designed experiments and analyzed data. P.H.T. designed and executed experiments and analyzed data. A.M.Q. and T.E.H. designed experiments and conceived the study. All authors wrote the manuscript.

Competing interests
The authors declare no competing interests.

Additional information
Supplementary information is available for this paper at https://doi.org/10.1038/s41598-020-58421-9.

Correspondence and requests for materials should be addressed to S.R.J.H. or T.E.H.

Reprints and permissions information is available at www.nature.com/reprints.

Publisher's note Springer Nature remains neutral with regard to jurisdictional claims in published maps and institutional affiliations.